



A Journal of the Gesellschaft Deutscher Chemiker

Angewandte Chemie

GDCh

International Edition

www.angewandte.org

Accepted Article

Title: Molecular Mimics of Heterogeneous Metal Phosphides: Thermochemistry, Hydride-Proton Isomerism, and HER Reactivity

Authors: Joshua A. Buss, Masanari Hirahara, Yohei Ueda, and Theodor Agapie

This manuscript has been accepted after peer review and appears as an Accepted Article online prior to editing, proofing, and formal publication of the final Version of Record (VoR). This work is currently citable by using the Digital Object Identifier (DOI) given below. The VoR will be published online in Early View as soon as possible and may be different to this Accepted Article as a result of editing. Readers should obtain the VoR from the journal website shown below when it is published to ensure accuracy of information. The authors are responsible for the content of this Accepted Article.

To be cited as: *Angew. Chem. Int. Ed.* 10.1002/anie.201808307
Angew. Chem. 10.1002/ange.201808307

Link to VoR: <http://dx.doi.org/10.1002/anie.201808307>
<http://dx.doi.org/10.1002/ange.201808307>

COMMUNICATION

Molecular Mimics of Heterogeneous Metal Phosphides: Thermochemistry, Hydride-Proton Isomerism, and HER Reactivity

Joshua A. Buss, Masanari Hirahara, Yohei Ueda, and Theodor Agapie*

Abstract: A new series of low-valent dinuclear molybdenum complexes bearing phosphido or phosphinidene bridging ligands was synthesized as a structural model of heterogeneous metal phosphide catalysts. Addition of acid to a monocationic $\text{Mo}_2\text{-}\mu\text{-P}$ complex results in phosphide protonation, affording a dicationic $\text{Mo}_2\text{-}\mu\text{-PH}$ species. Alternatively, reaction of an isoelectronic $\text{Mo}_2\text{-}\mu\text{-P}$ precursor with LiBEt_3H gives a $\text{Mo}_2\text{H-}\mu\text{-P}$ complex. Mixing these species, one bearing a Mo-H and the other a P-H bond results in facile H_2 production at room temperature.

Heterogeneous metal pnictogenides represent a diverse class of solid-state materials with applications ranging from optoelectronics^[1] to reductive catalysis.^[2] With respect to the latter, transition metal phosphides have demonstrated high activities and stabilities in solar-fuels relevant catalyses^[3] such as HER ($2\text{H}^+ + 2\text{e}^- \rightarrow \text{H}_2$)^[2b,4] and ORR ($\text{O}_2 + 4\text{e}^- + 4\text{H}^+ \rightarrow 2\text{H}_2\text{O}$)^[2a,4a] with overpotentials and lifetimes that rival state of the art platinum catalysts.^[2b,4c] Despite this remarkable reactivity, the operative mechanism of these catalysts is not known.^[2b] Computation suggests that under HER conditions, both M- and P-protonation are viable pathways for generation of surface hydrogen adducts that, upon application of a reducing potential, can lead to formation of H_2 (Figure 1, top).^[5] While intense research has been devoted to understanding the nucleation and growth of metal pnictogenide nanocrystals, affording atomically precise pictures of these materials,^[6] homogenous models of bulk transition metal phosphides are scarce.

Transition metal phosphides are structurally diverse, with the stoichiometric or metal-rich phases displaying bridging phosphide building blocks.^[2b] This $\mu\text{-P}$ motif is likewise known for molecular metal phosphides; however, M-P-M linkages reported to date either feature high/mid oxidation state metals^[7] or largely asymmetric phosphide coordination^[8] (Figure 1, bottom). Dinuclear symmetric bridging phosphides have been demonstrated as intermediates in intermetal P-atom transfer reactions^[7c] and have been prepared by the activation of white phosphorous,^[7a] phosphine,^[7d,7e] and phosphides.^[7b] Capping reactive terminal phosphides with transition metal-based Lewis acidic fragments has been employed to stabilize the $\text{M}\equiv\text{P}$ moiety, resulting in asymmetric $\mu\text{-P}$ complexes.^[8c-e] The high-valent metal

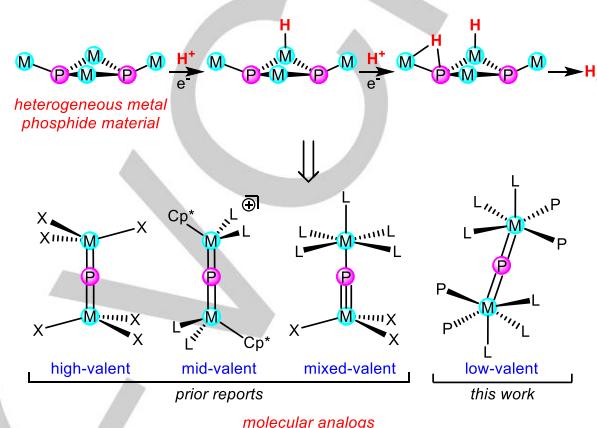
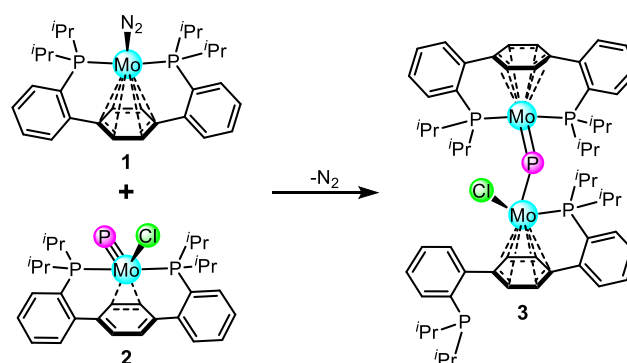


Figure 1. A representation of heterogeneous metal-phosphide catalysed HER (top) and classes of known molecular $\mu\text{-P}$ complexes (bottom).

maintains a short (ca. 2.15 Å) M-P distance, consistent with preservation of a formal triple bond.^[8a,8c] These complexes are not ideal models for HER chemistry by heterogeneous metal phosphide catalysts because of the propensity for protonolysis of supporting amide or alkoxide ligands. Furthermore, they are electronically distinct, as the oxidation states of these molecular compounds do not reflect the low oxidation states found in heterogeneous binary transition metal phosphides.

We recently reported the first examples of transition metal complexes with both terminal phosphide ligands and d-electrons (**2**, Scheme 1).^[9] Herein, we extend this molecular Mo pnictogenide chemistry, reporting the preparation of a series of low-valent $\mu\text{-P}$ complexes. These compounds model important steps in the proposed mechanism of



Scheme 1. Synthesis of a low-valent Mo-P-Mo core.

[*] J. A. Buss, M. Hirahara, Y. Ueda, and Prof. T. Agapie
Division of Chemistry and Chemical Engineering
California Institute of Technology, Pasadena, CA 91125 (USA)
E-mail: agapie@caltech.edu

Supporting information and the ORCID identification number(s) for the author(s) of this article can be found under:
<https://doi.org/10.1002/anie.xxxxxxxx>.

COMMUNICATION

heterogeneous HER and provide an experimental benchmark for the thermochemistry of a bridging phosphinidene P–H bond.

Addition of Mo(0) complex **1** to a solution of terminal metal phosphide **2** affords a new species with five distinct $^{31}\text{P}\{^1\text{H}\}$ NMR resonances, at 1161.0, 82.9, 73.7, 70.3, and -5.3 ppm. This spectral signature, consistent with a C_1 symmetric Mo–P–Mo structure (**3**, Scheme 1), was corroborated by the ^1H NMR spectrum, which showed eight discrete resonances for the central arene protons between 3.5 and 5.5 ppm. Though the low-field ^{31}P signal in **3** resonates several hundred ppm downfield of diamagnetic symmetric or asymmetric bridging phosphide complexes,^[7a,8c] the $\mu\text{-P}$ assignment was conclusively established by XRD. The structure of **3** is dinuclear with a bridging phosphide ligand, one trans-spanning *para*-terphenyl diphosphine (*para*-P2) ligand, and one arm-on arm-off *para*-P2 unit (Figure 2). The Mo–P3 distances are similar for both metal centers (2.2831(3) (Mo1) and 2.2409(3) (Mo2) Å), most consistent with double bonds between both Mo ions and the $\mu\text{-P}$.^[7c] The chloride remains bound (2.5157(3) Å), prompting dissociation of one of the phosphine arms of the *para*-P2 ligand. Both arenes bind in an η^6 fashion with the Mo–arene contacts averaging 2.281(1) and 2.309(1) Å for Mo1 and Mo2, respectively.

A higher symmetry bridging phosphide was targeted via exchanging the chloride for a non-coordinating counterion (Scheme 2). Halide abstraction from **3** with one equiv. of $[\text{Na}][\text{BAR}^{\text{F}}_{24}]$ results in simpler NMR characteristics; the $^{31}\text{P}\{^1\text{H}\}$ NMR spectrum shows only two resonances at 1123.3 and 68.6 ppm in a 1:4 ratio, in accord with formation of **4**. Complex **4** crystallizes with C_2 symmetry (Figure 2). The $\mu\text{-P}$ ligand lies on a crystallographic special position, imposing equivalent M–P distances of 2.2747(2) Å, which agree well with related symmetric $\mu\text{-P}$ complexes bearing metal phosphide double bonds.^[7a,7c] The Mo η^6 -arene contacts in **4** are slightly elongated (2.301(2) Å,) when compared to the analogous fragment in **3**, potentially a consequence of steric congestion resulting from phosphine arm recoordination.

Stoichiometric reactions of **4** with the strong acid $[(\text{Et}_2\text{O})_2\text{H}][\text{BAR}^{\text{F}}_{24}]$ ($\text{BAR}^{\text{F}}_{24}$ = tetrakis[3,5-bis(trifluoromethyl)phenyl]borate)^[10] result in formation of a new species with four signals in the central arene region of the ^1H NMR spectrum—6.08, 5.74, 5.24, and 4.92 ppm—suggesting a C_s symmetric dinuclear solution structure. The $^{31}\text{P}\{^1\text{H}\}$ chemical shift for the terphenyl phosphines corroborate this assignment, resonating at 86.4 and 74.6 ppm. A third, low-field ^{31}P resonance is observed; a broad peak (1046.1 ppm, $\Delta f_{\text{FWHM}} = 112$ Hz) shifted 77 ppm upfield of the $\mu\text{-P}$ signal of **4** (Figure S21). Addition of $[(\text{Et}_2\text{O})_2\text{D}][\text{BAR}^{\text{F}}_{24}]$ to **4** forms the same species with a slightly shifted (1047.1 ppm) low-field resonance (Figures S21 and S24). Neither a new proton ($\text{HBAR}^{\text{F}}_{24}$) nor deuteron ($\text{DBAR}^{\text{F}}_{24}$) resonance was observed for this new complex; every observed ^1H NMR feature can be assigned and corresponds to the terphenyl diphosphine ligands. To our knowledge, only diamagnetic bridging phosphinidene ($\mu\text{-PH}$) complexes of the actinides have been prepared previously;^[11] the ^{31}P resonances are observed at 24.5 and 74.0 ppm, for the $\text{Th}_2\text{-}\mu\text{-PH}$ and $\text{U}_2\text{-}\mu\text{-PH}$ compounds, respectively.^[12] Terminal phosphinidenes supported by U and Zr and sterically protected by

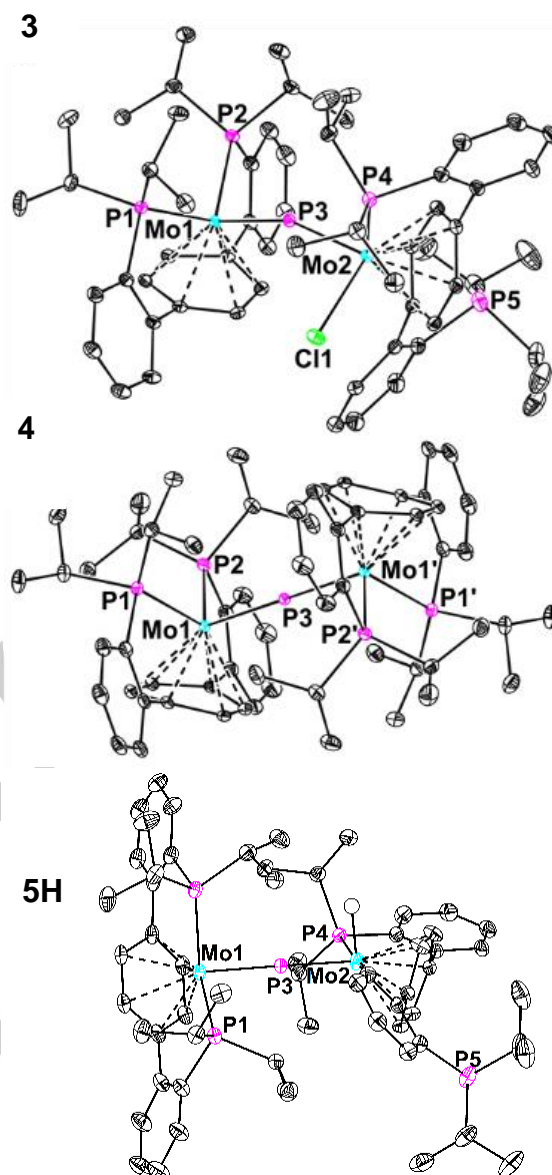
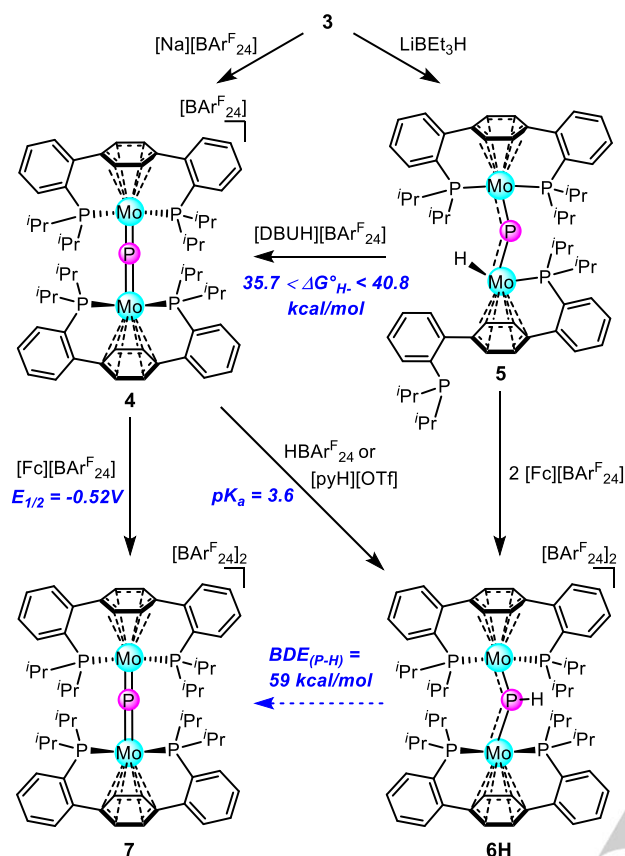


Figure 2. Solid-state structures of **3**, **4**, and **5H**. Protons and counterions (**4**) are omitted for clarity. Anisotropic thermal displacement ellipsoids are shown at a 50% probability level. Select bond distances [Å] and angles ($^\circ$): **3** – Mo1–P3: 2.2831(3), Mo2–P3: 2.2409(3), \angle Mo1–P3–Mo2 154.23(1); **4** – Mo1–P3 2.2747(2); **5H** – Mo1–P3 2.3250(4), Mo2–P3 2.2180(5), \angle Mo1–P3–Mo2 174.75(2).

bulky TREN variants were reported recently.^[13] The $^{31}\text{P}\{^1\text{H}\}$ chemical shifts for these PH moieties vary significantly, resonating at 2460 ppm for the U complex^[13b] and at 247 ppm for the Zr compound,^[13a] complicating phosphinidene assignment strictly on the basis of ^{31}P chemical shift. The chemical shift of the P-bound proton is likewise highly variable,^[13a,14] and in some of these complexes is (as in complex **6H**) not observed in the ^1H NMR.^[12,13b] IR spectra were collected for both **6H** and **6D** and no clear P–H stretch was observed.^[15] Despite this, the data, particularly the isotopic sensitivity of the $\mu\text{-P}$ $^{31}\text{P}\{^1\text{H}\}$ NMR resonance and the lack of a Mo hydride signal in the ^1H NMR, are

COMMUNICATION



Scheme 2. Reactivity and thermochemical parameters of P- and PH-bridged Mo_2 complexes.

most consistent with protonation of **4** at the phosphide, giving μ -phosphinidene **6H**.^[16] Efforts to crystallize **6H** uniformly resulted in formation of single crystals of a complex formally missing a hydrogen atom—dinuclear $\text{Mo(II)}-\mu\text{-P}-\text{Mo(III)}$, **7** (Figure S38). Dication **7** can be prepared independently by the one electron oxidation of **4** with $[\text{Fc}][\text{BARF}_{24}]$. The μ -phosphide in the solid-state structure of **7** (grown from a reaction of **4** with acid) lies on a symmetry special position, giving two equivalent $\text{Mo}-\text{P}$ distances of 2.276(1) Å. The independently synthesized sample (from single electron oxidation) crystallizes as an isoform of **7**; the unit cells differ but the $\text{Mo}-\text{P}_{\text{phosphide}}$ distances are consistent with those observed previously at 2.294 and 2.260 Å, corroborating the absence of a hydrogen atom and in close agreement with the $\text{Mo}-\text{P}_{\text{phosphide}}$ distances observed for **4**. The X-band CW EPR spectrum of **7** shows a broad rhombic signal centred at $g = 2.027$ (Figure S28), consistent with an $S = \frac{1}{2}$ species.^[17] The formation of **7** from protonation of **4** (via **6H**) is suggestive of an intermolecular H_2 evolution pathway.

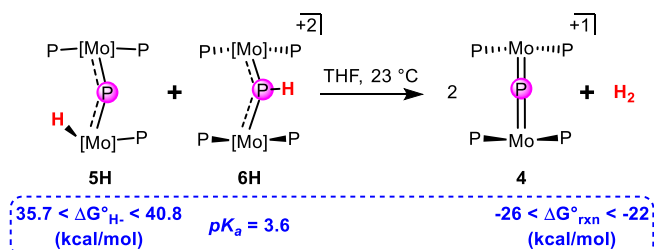
The conversion of **6H** to **7** represents the formal loss of a hydrogen atom, a mechanism proposed to be relevant to HER catalysis—the Volmer-Tafel pathway.^[4c,5] There is little experimental thermochemical data in the literature relevant to metal phosphide catalyzed HER,^[18] a shortcoming we sought to rectify. The cyclic voltammogram of **4** shows two reversible oxidation features (-0.52 V and 0.16 V), the former corresponding

to the $\text{Mo(II)Mo(II)}/\text{Mo(II)Mo(III)}$ couple, and one quasi-reversible reduction (-2.19 V) (Figure S25). With the standard potential for oxidation of **4** in hand, a $\text{p}K_{\text{a}}$ for phosphide protonation was required to complete a square-scheme for HAT from **6H** (Scheme 2, blue). Addition of pyridinium triflate to the THF solution of **4** displayed partial protonation of the $\mu\text{-P}$ motif (Figure S30). Acid titration afforded a $\text{p}K_{\text{a}}$ value for the bridging phosphide— 3.6 ± 0.1 in THF—the first observed value for the acidity of bridging phosphinidene. This starkly contrasts a reported $\text{Mn}_2-\mu\text{-PH}$ complex, in which the P-bound H-atom reacts as a hydride.^[7e] Calculating the $\text{BDE}_{(\text{P}-\text{H})}$,^[19] including a THF solvent correction,^[20] gives a value of 59 kcal/mol; this P–H bond is significantly weaker than those of phosphine ($\text{BDE H}_2\text{P}-\text{H} = 83.9 \pm 0.5$),^[21] methyl phosphine ($\text{BDE MeH}_2\text{P}-\text{H} = 77 \pm 3$),^[22] and comparable to that of diphosphine ($\text{BDE H}_2\text{PHP}-\text{H} = 61.2$).^[23] The P–H bond of **6H** is only slightly stronger than the S–H bond of $(\text{CpMo})_2(\text{S}_2\text{CH}_2)(\text{S})(\text{SH})$ (55 kcal/mol), a molecular catalyst for electrochemical HER.^[24]

It is notable that the most Brønsted-basic site of complex **4** is the $\mu\text{-P}$. In HER catalysis, the basicity of P atoms is invoked in forming surface bonded H-atoms; however, H adsorption at P is proposed to occur only after metal sites have been occupied.^[5,25] For comparison, a Mo hydride μ -phosphido was targeted by treating asymmetric **3** with 1 equiv. of LiBEt_3H . A new diamagnet with an apparent triplet at -1.55 ppm ($^2J(\text{P},\text{H}) = 17.0$ Hz)^[26] in the ^1H NMR spectrum was observed, in line with generation of **5** (Scheme 2). The $^{31}\text{P}\{^1\text{H}\}$ NMR spectrum shows four resonances (1057.4, 103.9, 69.5, and -4.4 ppm), indicating maintenance of the C_1 structure. The solid-state structure corroborates the solution spectroscopy, demonstrating an asymmetric dinuclear complex in which one diphosphine ligand is *trans*-spanning and the other adopts an arm-on arm-off binding motif (Figure 2). The $\text{Mo}-\mu\text{-P}$ distances remain relatively similar at 2.3250(4) and 2.2180(5) Å for the diphosphine and monophosphine coordinated Mo centers, respectively. These metrics suggest maintenance of the two $\text{Mo}=\text{P}$ double bonds^[7a,7c] following hydride installation.

Hydride **5H** represents a two-electron reduced isomer of phosphinidene **6H**. Interested in the potential to undergo a Mo-to-P H-shift, **5H** was oxidized with 2 equiv. of $[\text{Fc}][\text{BARF}_{24}]$ (Scheme 2). Multinuclear NMR spectroscopy shows moderate conversion to **6H** (39%), demonstrating the feasibility of this rearrangement. Hydride-proton isomerism has been discussed in the context of ligand non-innocence for transition metal catalyzed HER.^[27] Our results indicate that both phosphide and metal moieties can serve as sites for hydrogen binding. This process provides experimental precedent for the proposed “active role” of P-sites in HER^[28] and mimics the fluxionality proposed for surface adsorbed H-atoms.^[4c,29] Low-energy pathways have been determined computationally in which H-atoms migrate on the surface to promote H_2 evolution,^[30] a mobility mimicked in the conversion of **5H** to **6H**, albeit in an oxidative process. The inverse reaction, reduction of **6H** with 2 equiv. of CoCp_2 , however, formed **4**, presumably due to H_2 production upon reduction (a significantly weaker P–H bond is anticipated for a reduced Mo(I)Mo(II) bridging

COMMUNICATION



Scheme 3. H₂ evolution from well-defined Mo–H and P–H precursors.

phosphinidene). It is also possible that terphenyl diphosphine chelation prohibits reversion of **6H** to **4**.

With access to complexes with both Mo–H and P–H bonds, we sought to test for formation of H₂ (Scheme 3). Upon mixing THF solutions of **5H** and **6H**, consumption of both complexes and formation of monocationic complex of **4** was observed (Figure S33). Monitoring the reaction over time showed good material balance; the sum of the three dinuclear complexes, **4**, **5H**, and **6H**, remained relatively constant (Figure S33), though the previously characterized mononuclear dihydride^[31] [P₂MoH₂] was also detected as a minor product. These data are consistent with a binuclear hydrogen production pathway between **5H** and **6H**. The evolved H₂ was sequestered with an organometallic rhodium complex, [Rh(^tBu₂xanPOP)Cl] (^tBu₂xanPOP = 4,5-bis(di-tert-butylphosphino)-9,9-dimethyl-9H-xanthene), via the formation of *cis* dihydride complex, *cis*-[Rh(^tBu₂xanPOP)(H)₂Cl] (Figure S34).^[32] The hydricity of **5H** was bracketed by reactions with a series of acids (Figure S52), falling between 35.7 and 40.8 kcal/mol. The relatively strong hydricity of **5H** is in agreement with the observed facile H₂ production; the reaction free energy for protonation of **5H** by **6H** is between -22 and -26 kcal/mol.^[33]

In summary, we have synthesized a new series dinuclear metal phosphides that model elementary steps proposed for heterogeneous metal phosphide HER catalysts. With a conserved *para*-terphenyl diphosphine ancillary ligand set, both Mo₂ μ-PH and Mo₂ monohydride μ-P complexes were characterized. From the former, the bond dissociation enthalpy of the P–H was determined, giving a weak bond strength consistent with the observation of slow intermolecular H₂ evolution. From the latter, oxidation results in a Mo–H to P–H isomerization, mimicking the fluxionality proposed for surface adsorbed H-atoms.^[4c] Mixing these species, **5H** and **6H**, results in facile H₂ formation under ambient conditions in a demonstration of stoichiometric HER with a molecular metal phosphide.

Acknowledgements

We thank Lawrence M. Henling and Dr. Mike Takase for crystallographic assistance and Dr. David VanderVelde for NMR expertise. T.A. is grateful for a Dreyfus fellowship, J.A.B. for an NSF graduate research fellowship, M.H. for funding from the Grant-in-Aid for Young Scientists (B) (17K18433), and Y.U. for financial support from the JSPS Research Fellowships for Young Scientists. This research was supported by the NSF, grant

number CHE-1151918 (T.A.), the Dow Next Generation Fund, and Caltech.

Keywords: μ-Phosphide • μ-Phosphinidene • Thermochemistry • Proton Reduction • Molybdenum

- [1] a) B. A. Glassy, B. M. Cossairt, *Small* **2017**, *13*, 1702038; b) S. Tamang, C. Lincheneau, Y. Hermans, S. Jeong, P. Reiss, *Chem. Mater.* **2016**, *28*, 2491-2506; c) M. Green, *Curr. Opin. Solid State Mater. Sci.* **2002**, *6*, 355.
- [2] a) A. Dutta, N. Pradhan, *J. Phys. Chem. Lett.* **2017**, *8*, 144; b) J. F. Callejas, C. G. Read, C. W. Roske, N. S. Lewis, R. E. Schaak, *Chem. Mater.* **2016**, *28*, 6017; c) S. Carencu, D. Portehault, C. Boissière, N. Mézailles, C. Sanchez, *Chem. Rev.* **2013**, *113*, 7981; d) A.-M. Alexander, J. S. J. Hargreaves, *Chem. Soc. Rev.* **2010**, *39*, 4388; e) S. T. Oyama, T. Gott, H. Zhao, Y.-K. Lee, *Catal. Today* **2009**, *143*, 94; f) S. T. Oyama, *J. Catal.* **2003**, *216*, 343.
- [3] a) H. B. Gray, *Nat. Chem.* **2009**, *1*, 7; b) N. S. Lewis, D. G. Nocera, *Proc. Natl. Acad. Sci. USA* **2006**, *103*, 15729.
- [4] a) F. Yu, H. Zhou, Y. Huang, J. Sun, F. Qin, J. Bao, W. A. Goddard, S. Chen, Z. Ren, *Nat. Commun.* **2018**, *9*, 2551; b) Y. Shi, B. Zhang, *Chem. Soc. Rev.* **2016**, *45*, 1529; c) P. Xiao, W. Chen, X. Wang, *Adv. Energy Mater.* **2015**, *5*, 1500985; d) P. C. K. Vesborg, B. Seger, I. Chorkendorff, *J. Phys. Chem. Lett.* **2015**, *6*, 951.
- [5] P. Liu, J. A. Rodriguez, *J. Am. Chem. Soc.* **2005**, *127*, 14871.
- [6] a) M. R. Friedfeld, J. L. Stein, B. M. Cossairt, *Inorg. Chem.* **2017**, *56*, 8689; b) B. M. Cossairt, *Chem. Mater.* **2016**, *28*, 7181; c) D. C. Gary, S. E. Flowers, W. Kaminsky, A. Petrone, X. Li, B. M. Cossairt, *J. Am. Chem. Soc.* **2016**, *138*, 1510.
- [7] a) J.-P. F. Cherry, F. H. Stephens, M. J. A. Johnson, P. L. Diaconescu, C. C. Cummins, *Inorg. Chem.* **2001**, *40*, 6860; b) M. Scheer, J. Müller, M. Schiffer, G. Baum, R. Winter, *Chem. Eur. J.* **2000**, *6*, 1252; c) M. J. A. Johnson, P. M. Lee, A. L. Odom, W. M. Davis, C. C. Cummins, *Angew. Chem. Int. Ed.* **1997**, *36*, 87; d) M. C. Fermin, J. Ho, D. W. Stephan, *J. Am. Chem. Soc.* **1994**, *116*, 6033; e) A. Strube, J. Heuser, G. Huttner, H. Lang, *J. Organomet. Chem.* **1988**, *356*, C9.
- [8] a) G. Balázs, L. J. Gregoriades, M. Scheer, *Organometallics* **2007**, *26*, 3058; b) M. E. García, V. Riera, M. A. Ruiz, D. Sáez, H. Hamidov, J. C. Jeffery, T. Riis-Johannessen, *J. Am. Chem. Soc.* **2003**, *125*, 13044; c) M. Scheer, P. Kramkowski, K. Schuster, *Organometallics* **1999**, *18*, 2874; d) M. Scheer, J. Müller, M. Häser, *Angew. Chem. Int. Ed.* **1996**, *35*, 2492; e) P. Kramkowski, G. Baum, U. Radius, M. Kaupp, M. Scheer, *Chem. Eur. J.* **1999**, *5*, 2890.
- [9] J. A. Buss, P. H. Oyala, T. Agapie, *Angew. Chem. Int. Ed.* **2017**, *56*, 14502.
- [10] M. Brookhart, B. Grant, A. F. Volpe, *Organometallics* **1992**, *11*, 3920.
- [11] For diamagnetic bridging phosphinidenes, see: a) Wildman, E. P.; Balázs, G.; Wooles, A. J.; Scheer, M.; Liddle, S. T. *Nat. Commun.* **2016**, *7*, 12884; b) Duttera, M. R.; Day, V. W.; Marks, T. J. *J. Am. Chem. Soc.* **1984**, *106*, 2907. For paramagnetic examples, refer to: a) K. F. Hirsekorn, A. S. Veige, P. T. Wolczanski, *J. Am. Chem. Soc.* **2006**, *128*, 2192; b) P. Sekar, M. Scheer, A. Voigt, R. Kirmse, *Organometallics* **1999**, *18*, 2833; c) A. Herrmann Wolfgang, B. Koumbouris, E. Herdtweck, L. Ziegler Manfred, P. Weber, *Chem. Ber.* **1987**, *120*, 931.
- [12] E. P. Wildman, G. Balázs, A. J. Wooles, M. Scheer, S. T. Liddle, *Nat. Commun.* **2016**, *7*, 12884.
- [13] a) H. Stafford, T. M. Rookes, E. P. Wildman, G. Balázs, A. J. Wooles, M. Scheer, S. T. Liddle, *Angew. Chem. Int. Ed.* **2017**, *56*, 7669; b) B. M. Gardner, G. Balázs, M. Scheer, F. Tuna, E. J. L. McInnes, J. McMaster, W. Lewis, A. J. Blake, S. T. Liddle, *Angew. Chem. Int. Ed.* **2014**, *53*, 4484.
- [14] M. R. Duttera, V. W. Day, T. J. Marks, *J. Am. Chem. Soc.* **1984**, *106*, 2907.
- [15] Relevant IR data for P–H/D bonds can be found in references 12-14.
- [16] We acknowledge that a Mo–H structure for **5H** cannot be explicitly ruled out; however, the preponderance of data supports a P–H assignment. A detailed discussion is provided in the Supplemental Information.

COMMUNICATION

- [17] M. J. Bezdek, S. Guo, P. J. Chirik, *Inorg. Chem.* **2016**, *55*, 3117.
- [18] For select examples of computationally derived P–H thermochemistry, see: a) Laursen, A. B.; Wexler, R. B.; Whitaker, M. J.; Izett, E. J.; Calvino, K. U. D.; Hwang, S.; Rucker, R.; Wang, H.; Li, J.; Garfunkel, E.; Greenblatt, M.; Rappe, A. M.; Dismukes, G. C. *ACS Catalysis* **2018**, *8*, 4408; b) Wexler, R. B.; Martirez, J. M. P.; Rappe, A. M. *ACS Catalysis* **2017**, *7*, 7718; c) Hansen, M. H.; Stern, L.-A.; Feng, L.; Rossmeisl, J.; Hu, X. *Phys. Chem. Chem. Phys.* **2015**, *17*, 10823; d) Ariga, H.; Kawashima, M.; Takakusagi, S.; Asakura, K. *Chem. Lett.* **2013**, *42*, 1481.
- [19] J. J. Warren, T. A. Tronic, J. M. Mayer, *Chem. Rev.* **2010**, *110*, 6961.
- [20] E. P. Cappellani, S. D. Drouin, G. Jia, P. A. Maltby, R. H. Morris, C. T. Schweitzer, *J. Am. Chem. Soc.* **1994**, *116*, 3375.
- [21] a) J. Berkowitz, G. B. Ellison, D. Gutman, *J. Phys. Chem.* **1994**, *98*, 2744; b) J. Berkowitz, L. A. Curtiss, S. T. Gibson, J. P. Greene, G. L. Hillhouse, J. A. Pople, *J. Chem. Phys.* **1986**, *84*, 375.
- [22] S. Berger, J. I. Brauman, *J. Am. Chem. Soc.* **1992**, *114*, 4737.
- [23] a) T. McAllister, F. P. Lossing, *J. Phys. Chem.* **1969**, *73*, 2996; b) For a tabulation of additional P–H BDEs, see: Luo, Y.-R. *Comprehensive Handbook of Chemical Bond Energies*; CRC Press: Boca Raton, FL, 2007.
- [24] A. M. Appel, D. L. DuBois, M. Rakowski DuBois, *J. Am. Chem. Soc.* **2005**, *127*, 12717.
- [25] a) P. Xiao, M. A. Sk, L. Thia, X. Ge, R. J. Lim, J.-Y. Wang, K. H. Lim, X. Wang, *Energy Environ. Sci.* **2014**, *7*, 2624; b) J. Tian, Q. Liu, N. Cheng, M. Asiri Abdullah, X. Sun, *Angew. Chem. Int. Ed.* **2014**, *53*, 9577.
- [26] The scalar coupling constants to both the bound phosphine and bridging phosphide are not resolved in the ¹H NMR spectrum, giving rise to an overlapping doublet of doublets.
- [27] L. M. A. Quintana, S. I. Johnson, S. L. Corona, W. Villatoro, W. A. Goddard, M. K. Takase, D. G. VanderVelde, J. R. Winkler, H. B. Gray, J. D. Blakemore, *Proc. Natl. Acad. Sci. USA* **2016**, *113*, 6409.
- [28] R. B. Wexler, J. M. P. Martirez, A. M. Rappe, *ACS Catal.* **2017**, *7*, 7718.
- [29] M. H. Hansen, L.-A. Stern, L. Feng, J. Rossmeisl, X. Hu, *Phys. Chem. Chem. Phys.* **2015**, *17*, 10823.
- [30] H. Ariga, M. Kawashima, S. Takakusagi, K. Asakura, *Chem. Lett.* **2013**, *42*, 1481.
- [31] J. A. Buss, G. A. Edouard, C. Cheng, J. Shi, T. Agapie, *J. Am. Chem. Soc.* **2014**, *136*, 11272.
- [32] M. C. Haibach, D. Y. Wang, T. J. Emge, K. Krogh-Jespersen, A. S. Goldman, *Chem. Sci.* **2013**, *4*, 3683.
- [33] E. S. Wiedner, M. B. Chambers, C. L. Pitman, R. M. Bullock, A. J. M. Miller, A. M. Appel, *Chem. Rev.* **2016**, *116*, 8655.

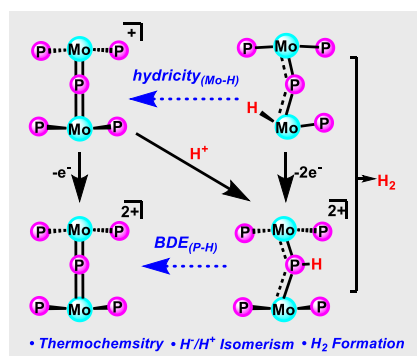
COMMUNICATION

Entry for the Table of Contents (Please choose one layout)

Layout 1:

COMMUNICATION

Molecularly Precise: A series of reduced dinuclear μ -phosphido complexes have been prepared as models for heterogeneous proton reduction catalysts. These molecular complexes provide insight into elementary reaction steps and thermochemical parameters relevant to their solid-state counterparts. μ -P protonation, Mo-to-P H-migration, and H-atom transfer have all been demonstrated, *en route* to H_2 formation.



Joshua A. Buss, Masanari Hirahara,
Yohei Ueda and Theodor Agapie*

Page No. – Page No.

**Molecular Mimics of Heterogeneous
Metal Phosphides: Thermochemistry,
Hydride-Proton Isomerism, and HER
Reactivity**